Protein Science (2000), *9*:2446–2456. Cambridge University Press. Printed in the USA.

Resonant mirror biosensor analysis of type Iα cAMP-dependent protein kinase B domain—Cyclic nucleotide interactions

WALLACE W. MUHONEN AND JOHN B. SHABB

Department of Biochemistry and Molecular Biology, University of North Dakota School of Medicine, Grand Forks, North Dakota 58202

(RECEIVED April 19, 2000; FINAL REVISION September 1, 2000; ACCEPTED September 18, 2000)

Abstract

A resonant mirror biosensor was used to study cyclic nucleotide–receptor interactions. In particular, a novel method was developed to determine inhibition constants (K_i) from initial rates of ligate association to immobilized ligand. This approach was applied to the comparison of cyclic nucleotide-binding properties of the wild-type isolated B domain of the cAMP-dependent protein kinase type Iα regulatory subunit and its Ala-334-Thr (A334T) variant that has altered cyclic nucleotide specificity. A cUMP-saturated form of the B domain was used for all measurements. Under the conditions used, cUMP did not affect the kinetics of B domain association to immobilized cAMP. Triton X-100 was required to stabilize the protein at nanomolar concentrations. The association and dissociation rate constants for wild-type and A334T B domains yielded equilibrium dissociation constants of 11 and 16 nM. Heterogeneity of ligate and immobilized ligand, mass transport effects, and other factors were evaluated for their influence on biosensor-determined kinetic constants. Biosensor-determined relative inhibition constants ($K_i' = K_i^{cAMP}/K_i^{analog}$) for 16 cyclic nucleotide analogs correlated well with those determined by a [^{3}H]cAMP binding assay. Previously published K_i' values for the B domain in the intact regulatory subunit were similar to those of the isolated B domain. The K_i' values for the wild-type and A334T B domains were essentially unchanged except for dramatic enhancements in affinity of cGMP analogs for the A334T B domain. These observations validate the isolated B domain as a simple model system for studying cyclic nucleotide–receptor interactions.

Keywords: cAMP-dependent protein kinase; biosensors; cyclic AMP; cyclic GMP; cyclic nucleotide analogs; kinetic analysis; inhibition constants

The extensively characterized cyclic nucleotide binding characteristics of the regulatory subunit (RIα) of cAMP-dependent protein kinase (reviewed in Beebe & Corbin, 1986), and the availability of the crystal structure of its cAMP-binding domains (Su et al., 1995) make this protein an excellent system for understanding the molecular basis for cyclic nucleotide binding selectivities of protein kinases. Information gained from this system has been transferable to other proteins that contain homologous cyclic nucleotide-binding domains. For example, mutation of a single alanine to a threonine in each of the cAMP-binding A and B domains of RIα dramatically increased their affinities for cGMP without affecting cAMP interaction (Shabb et al., 1990, 1991). Subsequent mutations of corresponding threonine residues to alanines in the bovine rod cyclic nucleotide-gated channel (Altenhofen et al., 1991) and the A and B domains of cGMP-dependent protein kinase (Reed et al., 1996) resulted in decreases in cGMP binding affinity without affecting cAMP interaction.

The presence in RIα of tandem cyclic nucleotide binding domains (A and B) that have subtle, yet distinct kinetic properties (Rannels & Corbin, 1980; Døskeland & Øgreid, 1984) and binding selectivities (Døskeland et al., 1983; Øgreid et al., 1989) complicates the study of cyclic nucleotide interactions with this protein. Initial studies of a soluble recombinant isolated RIα B domain point to its utility as a simpler model system for studying cyclic nucleotide–receptor interactions (Shabb et al., 1995; Kapphahn & Shabb, 1997).

Further characterization of the isolated B domain of RIα is presented in this study, validating it as a simple model system for studying cyclic nucleotide–receptor interactions. This is accomplished using resonant mirror biosensor technology as a non-isotopic kinetic approach to the study of small ligand–receptor interactions. In particular, a novel method is introduced for determining inhibition constants using initial rates of receptor association to immobilized ligand. The approach is applied to the

Reprint requests to: John B. Shabb, Department of Biochemistry and Molecular Biology, University of North Dakota School of Medicine, Grand Forks, North Dakota 58202-9037; e-mail: jshabb@medicine.nodak.edu.

comparison of cyclic nucleotide-binding selectivities of the wild-type isolated RIα B domain and its Ala-334-Thr (A334T) variant that has altered cGMP binding characteristics.

Results

General properties of the cUMP-saturated isolated B domain

The use of cAMP- or cIMP-bound B domain preparations for the biosensor measurements resulted in slow k_{on} values that were similar to the rates of dissociation of cAMP and cIMP from the B domain (not shown). To attain more accurate k_{on} values, cAMP and cIMP were exchanged with cUMP, which has an affinity for B domain that is two orders of magnitude less than that of cAMP. Residual cUMP in the B domain preparations did not appear to affect the kinetics of association of the B domain with immobilized AHA-cAMP at B domain concentrations used for biosensor measurements (35 nM or less). This was evidenced by the lack of effect of up to 100 nM of exogenously added cUMP on the initial rate of B domain association to immobilized AHA-cAMP (not shown).

Although cUMP-saturated B domain was stable at concentrations of 100 nM or greater, dilution of cUMP-saturated B domain to 10 nM resulted in rapid inactivation (Fig. 1). The instability was not due to the loss of bound cUMP because the rate of inactivation was unaffected by the addition of cUMP. Addition of 0.01% Triton X-100, however, completely protected 10 nM B domain from inactivation for up to 17 h of incubation at room temperature. Therefore, Triton X-100 was included in all subsequent experiments.

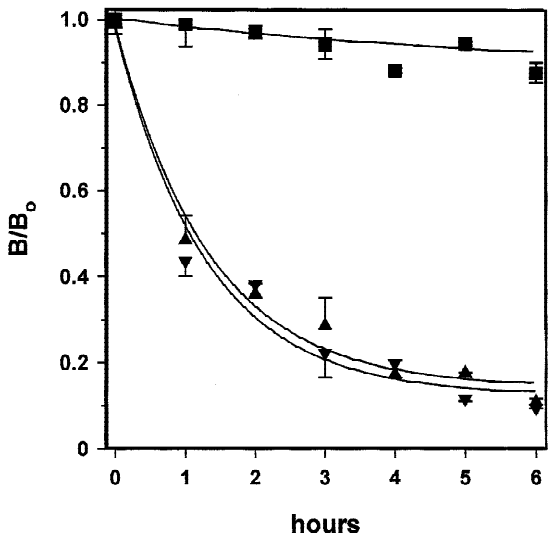

Fig. 1. Detergent stabilization of the isolated B domain. An aliquot of 19 μM cUMP-saturated B domain was diluted to 10 nM in 10 mM potassium phosphate, pH 6.8, 1 mM EDTA, 2 mM 2-mercaptoethanol in the presence of 0.01% Triton X-100 (squares) or 3.6 μM cUMP (downward triangles) or with no other addition (upward triangles). The samples were incubated at room temperature. The amount of remaining active B domain was measured at 1 h intervals on the IAsys by determining the initial rate of association of isolated B domain with immobilized AHA-cAMP. Data are plotted as the fraction of B domain remaining at time t (B/B_o). At time zero, initial rates of B domain association were 0.299, 0.255, and 0.785 arc-s/s for the + Triton X-100, + cUMP and no addition experiments, respectively. A twofold or greater enhancement of cAMP-binding activity was consistently observed in the presence of Triton X-100 and was independent of the B domain concentration or the assay method.

Characterization of isolated B domain interaction with immobilized AHA-cAMP

The 8-aminohexylamino analog of cAMP (AHA-cAMP) was selected as the analog to immobilize to the carboxymethyldextran cuvette because it is routinely cross-linked to cyanogen bromide-activated Sepharose for the affinity purification of cAMP-dependent protein kinase regulatory subunits (Dills et al., 1979). Recently, others have used this same analog to prepare a cAMP surface for capturing R subunit isoforms to study PKA anchoring protein interactions by surface plasmon resonance (Herberg et al., 2000). The extreme stability of the single-well cuvette allowed for the careful assessment of the cuvette system for determining kinetic parameters of B domain-cyclic nucleotide interactions.

A typical association of B domain with immobilized AHA-cAMP is shown in Figure 2. Data accumulated over an extended period of time (e.g., 10 min) yielded a k_{on} that fits best with double-phase as opposed to single-phase kinetics (Fig. 2A,B). The association curve could be fitted to a single-phase k_{on} when analysis was limited to the first 90 s of accumulated data (Fig. 2C). Because k_a^{on} and k_d^{on} values were similar whether they were calculated from double- or single-phase k_{on} values, the more convenient single-phase determinations were used for all subsequent measurements. Alternatively, the $k_a^{dR/dt}$ was determined from plots of initial rate (dR/dt) measurements vs. B domain concentration (Edwards & Leatherbarrow, 1997). Twenty seconds of accumulated association data was usually sufficient to establish an accurate initial rate using linear regression (Fig. 2D). As a rule, initial rate calculations gave more consistent values, particularly at low B domain concentration.

Although the dissociation of the B domain is first order (Shabb et al., 1995), the biosensor dissociation data fit a double-phase curve-fitting algorithm (Fig. 3). The minor fast-dissociating component (less than 20%) was attributed to dissociation of nonoptimally or nonspecifically bound B domain. Artifactual rebinding of the B domain during the dissociation phase was effectively eliminated by including 60 μM cAMP in the chase buffer. Therefore, only the slow component k_d^{diss} was evaluated.

The relationship between the k_{on} and B domain concentration was biphasic, with a break occurring at 20–35 nM (Fig. 4). Replotting the same data to give initial rate vs. the B domain concentration gave similar results. Because of the biphasic nature of the k_{on} data, kinetic constants were calculated for high (>20 nM) and low (<20 nM) ligate concentrations (Table 1). The kinetic parameters derived from k_{on} measurements at a low B domain concentration more closely met the self-consistency criteria of Schuck and Minton (1996b): (1) the K_d^{kin} was approximately equal to the K_d^{eq}; (2) k_d^{on} was approximately equal to k_d^{diss}, and (3) the k_{on} at every concentration of the B domain used was greater than the k_d^{on} (e.g., compare the y intercept to data points in Fig. 4). The deviation from pseudo-first-order kinetics was best explained by site heterogeneity on the cuvette surface, with the kinetics at the lower B domain concentrations best representing the solution properties of the protein (Edwards et al., 1995; O'Shannessy & Winzor, 1996; Bowles et al., 1997). The low range constants were therefore taken as more accurately representing the solution properties of the B domain.

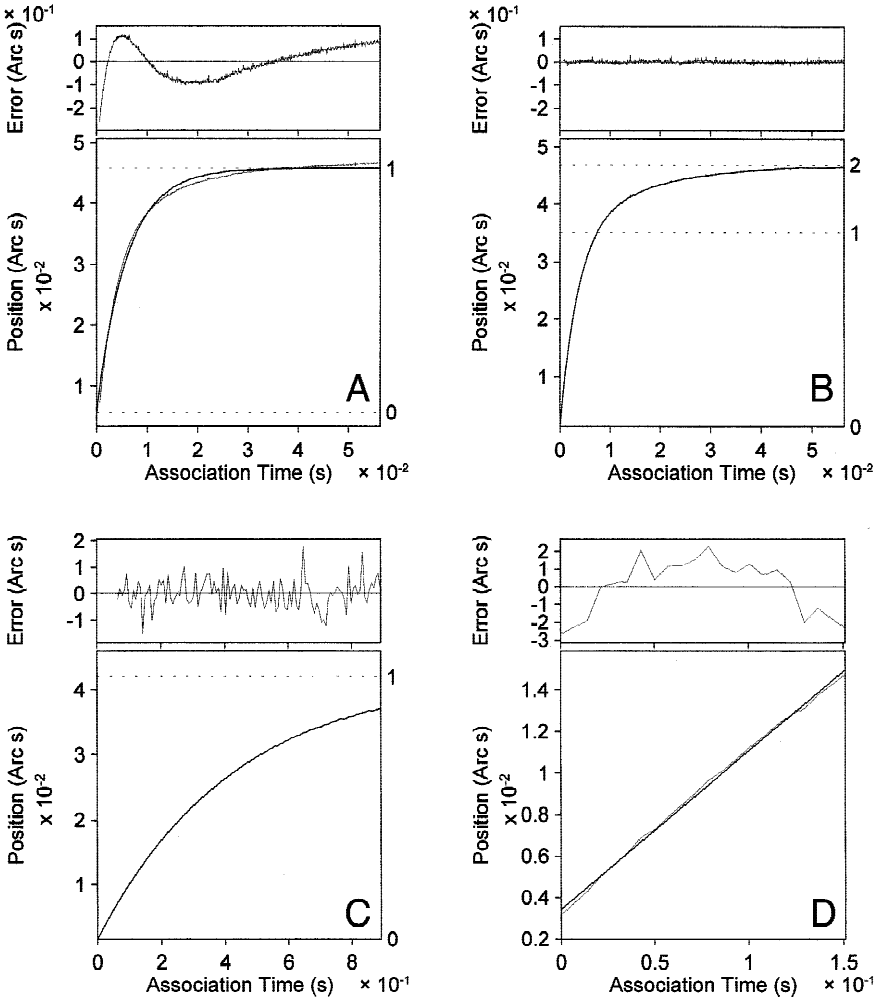

Fig. 2. Modeling of B domain association with immobilized AHA-cAMP. Binding of 90 nM wild-type isolated B domain to immobilized AHA-cAMP was monitored for 550 s at 30 °C with a single-well IAsys cuvette as described in Materials and methods. The numbered, dashed lines in each of the association plots indicate the extents of association for the first and second phases. The top graph of each panel is a plot of the residual errors of calculated vs. experimental data. **A:** Monophasic curve-fitting of the entire dataset. **B:** Biphasic curve-fitting of the entire dataset. The calculated maximum extent of binding for the first and second phases were 326 and 114 arc-s. **C:** Monophasic curve fitting of the first 90 s of accumulated data. The calculated maximum extent of binding was 391 arc-s. **D:** Linear regression of the first 15 s of initial rate of association, the slope of which is dR/dt.

The influence of mass transport on k_a determinations was also evaluated because under certain conditions k_a values can be severely underestimated (Karlsson et al., 1993; Nieba et al., 1996; Schuck & Minton, 1996a; Myszka et al., 1997; Schuck, 1997). Furthermore, others have shown mass transport limitation for the association of the PKA regulatory subunit to immobilized cAMP in the BIAcore surface plasmon resonance biosensor (Herberg & Zimmermann, 1999). A convenient and accepted test for detecting mass transport is to determine the effect on the k_{on} of flow rate over the surface of the immobilized ligand (Myszka et al., 1997). In the IAsys, flow rate in the cuvette is controlled by the stirrer amplitude. The data in Figure 5 demonstrated that the initial rate of B domain association steadily increased up to a stirrer setting of 80, but remained essentially constant at stirrer settings greater than 80. The density of immobilized AHA-cAMP had very little if any influence on the minimum stirrer setting required for achieving a stable initial rate. Because all experiments were done at a stirrer setting of 100, all association data were attributed to interaction kinetics between B domain and immobilized AHA-cAMP and not to mass transport-limited kinetics. Other evidence that mass transport was not a factor include the relative insensitivity of k_a values determined with immobilized AHA-cAMP cuvettes of varying density (not shown) and the linear relationship between the k_{on} and B domain concentration even in the low nM range (e.g., Fig. 4).

As Table 1 indicates, the K_d values are similar for the wild-type and A334T B domains, indicating that the Ala-to-Thr mutation has a minimal effect on the binding affinity of the B domain to immobilized AHA-cAMP. It is not clear what might account for the biphasic nature of the k_{on} data, but the difference in K_d values for high and low protein ranges for either wild-type or A334T B domain differed only by a factor of 2.

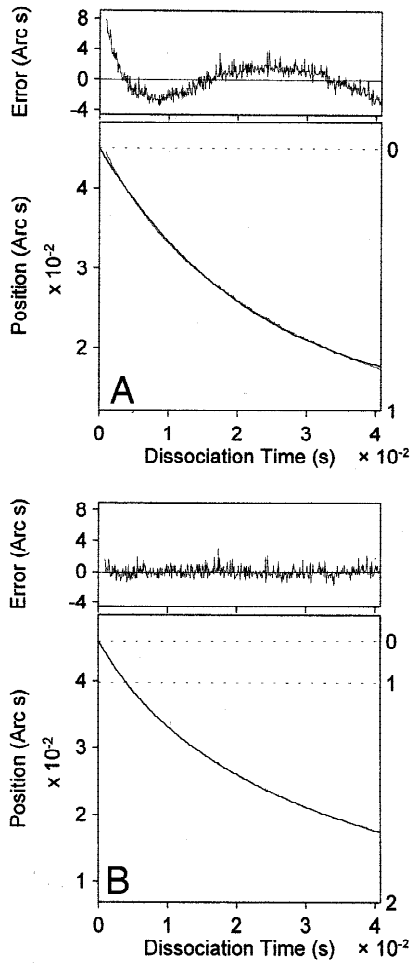

Fig. 3. Modeling of B domain dissociation with immobilized AHA-cAMP. After 9 min of association of 90 nM wild-type isolated B domain to a single-well immobilized AHA-cAMP cuvette at 30 °C, the dissociation of B domain was monitored for 400 s in the presence of excess cAMP as described in Materials and methods. The numbered, dashed lines in each of the dissociation plots indicate the extents of dissociation for the first and second phases. The top graph of each panel is a plot of the residual errors of calculated vs. experimental data. **A:** Monophasic curve fitting of the entire dataset. **B:** Biphasic curve fitting of the entire dataset. The calculated extents of the first and second phase were 67 and 329 arc-s.

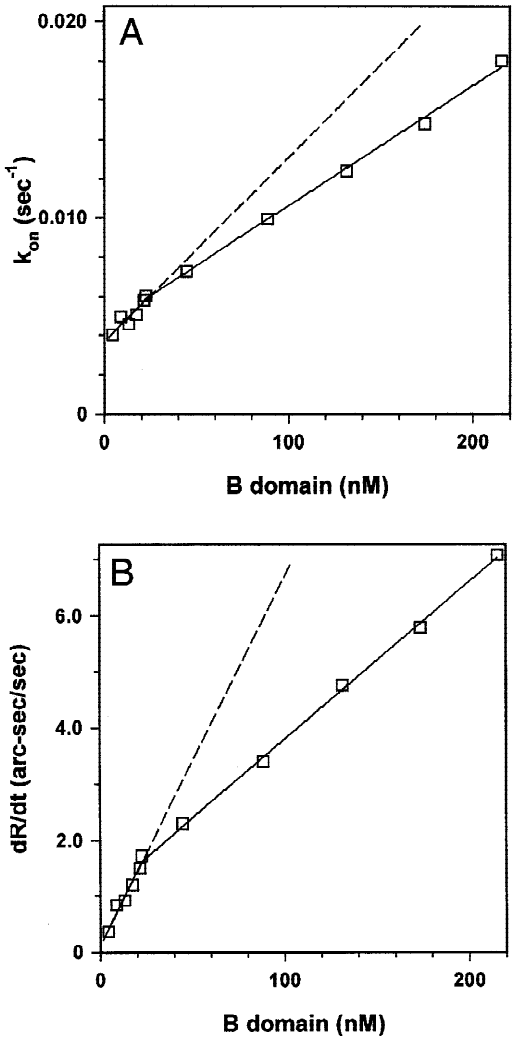

Fig. 4. Determination of rate constants for B domain interaction with immobilized AHA-cAMP using biosensor association data. This is an example of the experiments that were used to compile the kinetic data in Table 1. **A:** The k_{on} values were determined at increasing B domain concentrations as in Figure 2C. The slope and *y*-intercept of a linear regression of a plot of k_{on} vs. B domain yielded k_a^{on} and k_d^{on}, respectively. **B:** Initial rates (dR/dt) were calculated as in Figure 2D, using the same data as in **A**. Linear regression of dR/dt vs. B domain concentration yielded $k_a^{dR/dt}$. Both transformations of the association data (**A** and **B**) illustrate the deviation from pseudo-first-order kinetics of the association phase when examined over a wide protein concentration range. Linear regressions are for the high range (21–215 nM; solid lines) and low range (5–21 nM; dashed lines) of B domain concentration. This experiment was done with a single well cuvette at 30 °C.

Biosensor determination of inhibition constants

The determination of the inhibition constants of cAMP analogs was initially performed using the approach of Nieba et al. (1996), in which the K_i is determined from a plot of k_{on} vs. total inhibitor concentration using nonlinear regression. The determination of reliable k_{on} values proved to be problematic, however, for highly inhibited samples. This was due to the difficulty in accumulating sufficient association data that could be accurately fitted by the nonlinear regression. Although increasing the concentration of B domain in the assay minimized this problem, this also introduced unacceptable levels of cUMP into the assay.

As an alternative approach, initial association rates were used to calculate K_i values as described in Materials and methods. Accurate dR/dt values were easily obtained by linear regression of the first 20 to 60 s of accumulated association data even at high inhibitor concentrations. Typical initial rate data for the wild-type B domain with cAMP as the competitor nucleotide are shown in Figure 6A. The initial rates were then plotted against inhibitor concentration, and the K_i was determined by fitting the data to Equation 8. Figure 6B shows a typical inhibition curve of the B domain association rates in the presence of increasing cAMP. To calculate the K_i, k_aR_{max} values were fixed for a given B domain preparation and cuvette. Although the B domain concentration of the frozen stock concentrations was known, this parameter was kept as a variable to allow for minor changes in protein concentration due to slow inactivation of B domain stored at 4° over a

Table 1. *Kinetic constants for isolated B domains derived from biosensor k_{on} determinations*

B domain	Range[a]	$k_a^{dR/dt}$ ($s^{-1}M^{-1}$) ($\times 10^{-5}$)	k_a^{on} ($s^{-1}M^{-1}$) ($\times 10^{-5}$)	k_d^{on} (s^{-1}) ($\times 10^{3}$)	k_d^{diss} (s^{-1}) ($\times 10^{3}$)	K_d^{kin} (nM)[b]	K_d^{eq} (nM)
Wild-type (3)[c]	Low	1.7 ± 0.47	2.3 ± 0.44	2.3 ± 0.46	2.7 ± 0.33 (19)	11.3 ± 3.66	9.88 ± 3.44
Wild-type (8)	High	0.91 ± 0.14	1.2 ± 0.20	3.9 ± 0.46		37.0 ± 5.51	23.2 ± 3.61
A334T (12)	Low	2.7 ± 0.37	3.5 ± 0.55	3.9 ± 0.42	2.8 ± 0.13 (48)	16.0 ± 3.70	17.0 ± 4.45
A334T (10)	High	1.1 ± 0.25	1.4 ± 0.36	6.6 ± 1.1		60.6 ± 6.79	30.6 ± 4.25

[a]Low range experiments were with B domain concentrations between 1 and 35 nM. High range experiments were with B domain concentrations between 20 and 210 nM.
[b]The K_d^{kin} constants were calculated from k_d^{on} and k_a^{on}.
[c]Number of experiments for each B domain are indicated in parentheses. The $k_a^{dR/dt}$, k_a^{on}, k_d^{on}, and K_d^{eq} values were derived from the same set of association experiments. The k_d^{diss} values were calculated directly from dissociation experiments. No distinction was made between k_d^{diss} values obtained from high or low B domain concentrations.

period of days. The K_i was considered reliable if it was consistent with the inhibitor concentration at half-maximal *dR/dt* as determined by visual inspection, and if the fitted value for B domain concentration was in reasonable agreement with the concentration of B domain determined by [^{3}H]cAMP-binding activity.

Mapping of cyclic nucleotide interactions with the isolated wild-type and A334T B domains

Relative inhibition constants (K_i') for 16 different cyclic nucleotides were determined for the wild-type and A334T B domain by the initial rate method (Table 2) and compared with those derived from the [^{3}H]cAMP equilibrium binding assay. Linear regression of the K_i' values from the two methods (Fig. 7A) gave a slope of 1.17 ($r^2 = 0.839$). The biosensor assay therefore had a similar dynamic range and accuracy as the [^{3}H]cAMP equilibrium binding assay for determining K_i' values.

The biosensor K_i' values were next compared with previously published K_i' values for the B domain in the intact *R* subunit (Fig. 7B). The slope of 1.02 for the linear regression of the two sets of data ($r^2 = 0.891$) demonstrated that isolation of the B domain from the *R* subunit did not grossly affect the cyclic nucleotide binding specificity of the *R* subunit. Comparison of the [^{3}H]cAMP-binding K_i' values with those from the literature gave a slope of 0.82 ($r^2 = 0.882$) (not shown).

The A334T B domain K_i' values derived from the biosensor and [^{3}H]cAMP-binding methods were also compared (Fig. 7C). The 1.17 slope of the linear regression ($r^2 = 0.993$) was very similar to that for the wild-type B domain. The major change was in the positioning of the cGMP analogs (solid squares) relative to the other cyclic nucleotides. The selective disjunction of cGMP analog selectivity of the isolated A334T B domain is illustrated in Figure 7D. Linear regression of K_i' values for the wild-type and A334T B domains yielded a slope of 0.862 ($r^2 = 0.902$), excluding cyclic GMP analogs, which are clustered away from the other 12 cyclic nucleotides.

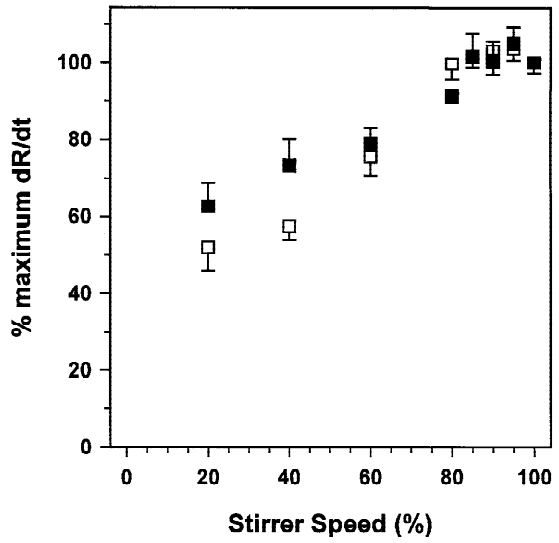

Fig. 5. Effect of stirrer setting on the rate of association of isolated B domain to immobilized AHA-cAMP. The initial rate of association was monitored in both wells of a dual well cuvette at given stirrer settings for 3 min at 25 °C followed by regeneration as described in Materials and methods. The process was repeated at random stirrer settings for a low density well (R_{max} = 195 arc-s; solid squares) and a higher density well (R_{max} = 650 arc-s; open squares). The experiment was done at a final B domain concentration of 4 nM in buffer A. Samples were diluted to the appropriate final concentration immediately before addition to the cuvette. Error bars are ± SEM (n = 4).

Discussion

The present study demonstrates that the isolated B domain is a useful model for studying cyclic nucleotide–receptor interaction. Kinetic constants for the B domain–cyclic nucleotide binding were readily determined with a resonant mirror biosensor. The 11 nM K_d of cAMP-binding to the isolated B domain was about 10-fold higher than the K_d for the B domain in intact RIα reported by others (Døskeland & Øgreid, 1984). This difference in affinity was due mainly to an order of magnitude lower k_a for the isolated B domain. The cause for the lowered affinity of the isolated B domain could be due to structural perturbations of its cAMP-binding pocket when it is separated from the rest of the *R* subunit, or it could be due to differences in the recognition of immobilized AHA-cAMP relative to cAMP in solution. The latter reason may also explain why the biosensor-determined dissociation rate constant of 0.0027 s^{-1} was somewhat greater than the 0.0017 s^{-1} that was previously determined by [^{3}H]cAMP dissociation from the isolated A334T B domain (Shabb et al., 1995). Given these dif-

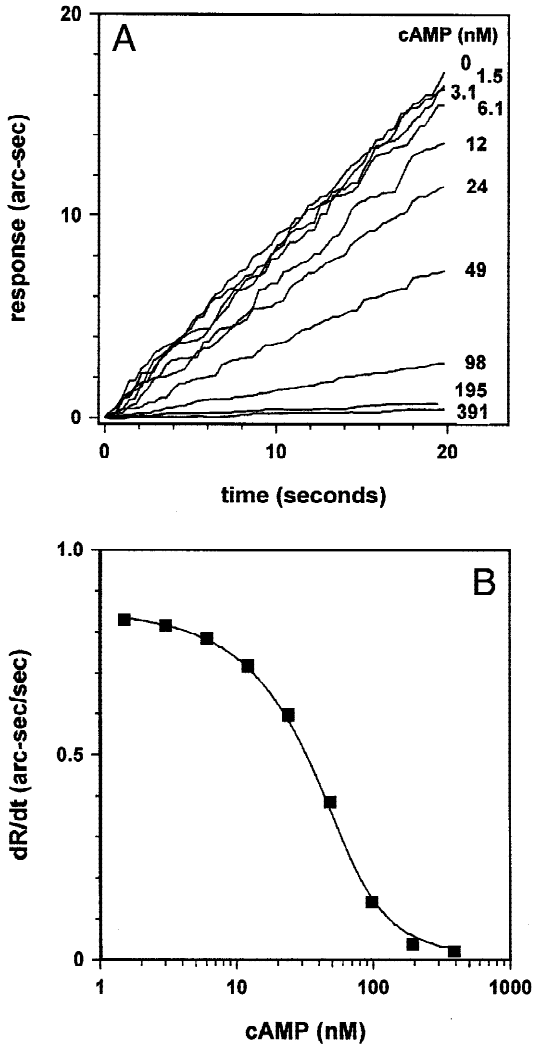

Fig. 6. Determination of a cyclic nucleotide inhibition constant using initial rates of B domain association to immobilized AHA-cAMP. **A:** Association of 15 nM isolated wild-type B domain was measured at 25 °C in a dual-well cuvette in the presence of increasing concentrations of competitor cAMP as described in Materials and methods. Data were accumulated at 0.2 s intervals. Shown are the initial 20 s of useable association data for each inhibitor concentration obtained after addition of the equilibrated protein-competitor nucleotide solution. The initial rate (dR/dt) was calculated as in Figure 2D. **B:** The K_i was determined by nonlinear regression of dR/dt with respect to total inhibitor concentration using Equation 8.

ferences, the biosensor data provided reasonable and believable kinetic constants for cAMP-B domain interactions.

The cyclic nucleotide binding selectivity of the B domain was generally unaffected when it was isolated from the rest of the RIα subunit (Fig. 7B). The overall pattern held regardless of whether inhibition constants were determined by the [^{3}H]cAMP-binding method or the initial rate method. The absolute ranking of the analogs was not identical, however. This could be due to experimental variation or to the differences in ligand used in the two methods. Inhibition constants derived from the initial rate method were more compressed than those obtained with the [^{3}H]cAMP-binding method resulting in correlation between the two sets of data that was greater than 1:1.

The biosensor was able to determine K_i values for very low affinity analogs much more effectively than was possible with the [^{3}H]cAMP-binding method. This was attributed to the fundamental differences in the methods themselves. The radioisotope method requires equilibration of the B domain and the competitor analog in the presence of 0.4 μM [^{3}H]cAMP to assess the fraction of B domain occupied by competitor. In the biosensor assay, however, the fraction of B domain that is occupied by competitor is determined by quantifying the amount of remaining unliganded B domain. The end result is that much higher analog concentrations are needed in the [^{3}H]cAMP-binding method to achieve the same degree of competitive inhibition in the initial rate method. Thus, the K_i for 2′-deoxy cAMP was not determined for the wild-type B domain with the [^{3}H]cAMP-binding assay because the extremely high concentration of nucleotide needed to inhibit [^{3}H]cAMP binding by 50% exceeded its solubility.

Mutation of Ala-334 to Thr did not affect the K_d of the isolated B domain for cAMP, providing direct proof that this mutation does not alter cAMP interaction. Previous studies inferred this conclusion through measurement of protein kinase activation and dissociation rate constants for cAMP (Shabb et al., 1990, 1991). The protein kinase activation constant is the concentration of cyclic nucleotide required for 50% activation of PKA holoenzyme and indirectly represents the mean affinity of the two cAMP binding sites. Activation constants were used in the same studies to demonstrate that the A334T B domain had a selective increase in affinity for cGMP analogs as compared to the wild-type R subunit (Shabb et al., 1990, 1991). The current study directly evaluates the cyclic nucleotide binding selectivity of the wild-type and A334T B domains through the determination of inhibition constants. The results clearly demonstrate that the change in cyclic nucleotide binding affinity was limited to a dramatically enhanced affinity for analogs having hydrogen bonding potential at the 2-amino position of cGMP.

Biosensor characterization of cyclic nucleotide interactions with intact RIα have not been attempted. Two kinetically distinct cAMP-binding sites per subunit, dimerization, and positive cooperativity between binding sites are all properties of the native protein that make this type of analysis problematic. Binding site heterogeneity and multivalence are recognized problems with respect to biosensor analysis (reviewed in Hall & Winzor, 1998), and investigators have tended to avoid these factors when possible (Kalinin et al., 1995). A compromise model would be the use of *R* subunits in which one or the other cAMP-binding site is mutated to eliminate cAMP-binding (reviewed in Shabb & Corbin, 1992), allowing characterization of the remaining functional site. This approach has yet to be tested.

Several approaches to determining inhibition constants using biosensor technology have been described. The approach described in this study is the latest and, in our hands, the most robust permutation of solution-based determination of kinetic constants using a biosensor. What distinguishes the current approach is the use of initial rates to directly extract a K_i based on the kinetic properties of the cyclic nucleotide-B domain interaction. Karlsson (1994) was the first to use initial rates to determine inhibition constants in solution, but this method relied on the initial rates being determined by mass transport, a condition that does not apply to the present study.

Others have exploited k_{on} to empirically (Hall & Winzor, 1997) or mechanistically (Nieba et al., 1996) determine inhibition constants. As described in Results, difficulties in accurately measuring

Table 2. *Relative inhibition constants of cyclic nucleotide analogs for the RIα B domain*[a]

Cpd	Cyclic nucleotide	Isolated wt-B domain, K_i'		Intact RI, K_i'	Isolated A334T-B domain, K_i'	
		[^{3}H]cAMP- binding	Initial rate	Literature values[b]	[^{3}H]cAMP-binding	Initial rate
1	8-methylamino cAMP	12	12	3.3[c]	8.4	4.6
2	8-aminohexylamino cAMP	3.8	1.2	1.6[c]	2.3	1.5
3	6-Cl cPuMP	1.1	2.5	0.60[d]	2.1	2.0
4	cAMP	1.0	1.0	1.0[c]	1.0	1.0
5	N^6-phenyl cAMP	0.31	1.1	0.48[c]	0.50	1.5
6	1, N^6 etheno cAMP	0.11	1.1[e]	0.11[c]	0.79	1.7
7	N^6-butyryl cAMP	0.047	0.36	0.093[c]	0.094	0.38
8	8-piperidino cAMP	0.025	0.21	0.065[c]	0.019	0.065
9	cIMP	0.023	0.16	0.024[c]	0.11	0.24
10	N^6-ethylamino cAMP	0.017	0.50[e]	—	0.034	0.17
11	8-amino cGMP	0.010	0.043	—	1.4	1.4
12	cGMP	0.0085	0.080	0.012[c]	2.5	2.2
13	1,N^2-β-D-phenyletheno cGMP	0.0072	0.083	0.0087[c]	7.9	2.3
14	cUMP	0.00049	0.0068	—	0.0054	0.036
15	2′-deoxy cAMP	0.00041	0.0013	0.00072[d]	0.00067	0.0013
16	2′-deoxy cGMP	N.D.	0.000046	—	0.0011	0.0019

[a]Relative inhibition constants (K_i') are expressed as K_i^{cAMP}/K_i^{analog}. Values were determined by either the [^{3}H]cAMP binding assay or the initial rate assay described in Materials and methods. The initial rate-determined K_i^{cAMP} was 25 nM for the isolated wt-B domain and 32 nM for the isolated A334T B domain. K_i' values are the means of at least three determinations except where footnoted. Standard errors of the mean did not exceed 25%.
[b]Literature values are for K_i' determinations of the B domain in the intact RIα subunit.
[c]Øgreid et al. (1989).
[d]De Wit et al. (1982).
[e]This K_i' value is the mean of duplicate determinations.

k_{on} at low ligate concentrations dampened enthusiasm for this method. In addition, use of initial rates instead of k_{on} minimized ligate depletion and the consequent invalidation of pseudo-first-order kinetics, a concern that has been raised with regard to the IAsys biosensor (Hall & Winzor, 1997; Hall et al., 1997).

Equilibrium approaches to determining inhibition constants similar to the ones described by others (Morelock et al., 1995; Mann et al., 1998) were also tried. Considerably more time was required for data accumulation with this approach. Furthermore, the instability of dilute solutions of B domain tended to complicate interpretation of association kinetics.

The resonant mirror biosensor provides a sensitive, reliable, and cost-effective alternative to radioisotope methods for the study of cyclic nucleotide–receptor interactions. The highly stable character of the immobilized cAMP cuvette significantly reduces expendable costs for the biosensor assay. This is in contrast to the high cost of purchase and disposal of [^{3}H]cAMP used in the traditional radioisotope assay. The biosensor assay also has some advantage in terms of time required to generate the raw data. This is especially true when initial rates are used to calculate inhibition constants. The methods used in this study should prove to have general applicability to small ligand–receptor interactions with the major challenge being the generation of an appropriately recognized and easily regenerated immobilized ligand.

Materials and methods

Materials

[2,8-^{3}H]cAMP (50 Ci/mmol) was from Amersham (Piscataway, New Jersey). Adenosine-3′,5′-cyclic monophosphate (cAMP), guanosine-3′,5′-cyclic monophosphate (cGMP), inosine-3′,5′-cyclic monophosphate (cIMP), uridine-3′,5′-cyclic monophosphate (cUMP), 2′-deoxyadenosine-3′,5′-cyclic monophosphate (2′-deoxy cAMP), 2′-deoxyguanosine-3′,5′-cyclic monophosphate (2′-deoxy cGMP), 8-methylaminoadenosine-3′,5′-cyclic monophosphate (8-methylamino cAMP), 8-aminohexylamino-3′,5′,-cyclic monophosphate (8-aminohexylamino cAMP), 6-chloropurine riboside-3′,5′-cyclic monophosphate (6-Cl cPuMP), N^6-monobutyryladenosine-3′,5′-cyclic monophosphate (N^6-monobutyryl cAMP), and 1, N^6-ethenoadenosine-3′,5′-cyclic monophosphate (1,N^6-etheno cAMP) were from Sigma (St. Louis, Missouri). 8-Piperidinoadenosine-3′,5′-adenosine cyclic monophosphate (8-Piperidino cAMP), N^6-phenyladenosine-3′,5′-cyclic monophosphate (N^6-phenyl cAMP), and β-phenyl-1,N^2-ethenoguanosine-3′,5′-cyclic monophosphate (PET-cGMP) were from BioLog (La Jolla, California). 8-Aminoguanosine-3′,5′-cyclic monophosphate (8-amino cGMP) was a gift from Jackie Corbin (Vanderbilt University). N^6-(2-aminoethyl) adenosine-3′,5′-cyclic monophosphate (N^6-ethylamino cAMP) was synthesized according to Dills et al. (1979).

Preparation of isolated wild-type and A334T B domains

Vectors encoding the 14,380 kDa isolated B domain of wild-type (WT) and A334T RIα were constructed as described previously (Shabb et al., 1995). The domains were expressed in *Escherichia coli* and purified to near homogeneity in a cIMP-saturated state by cAMP-affinity chromatography (Shabb et al., 1995). Aliquots containing 10 mM potassium phosphate, 1 mM ethylenediaminetetraacetic acid(EDTA), 0.01% Triton X-100 pH 6.8 were frozen in liquid nitrogen and stored at −70 °C. Protein stored in this manner

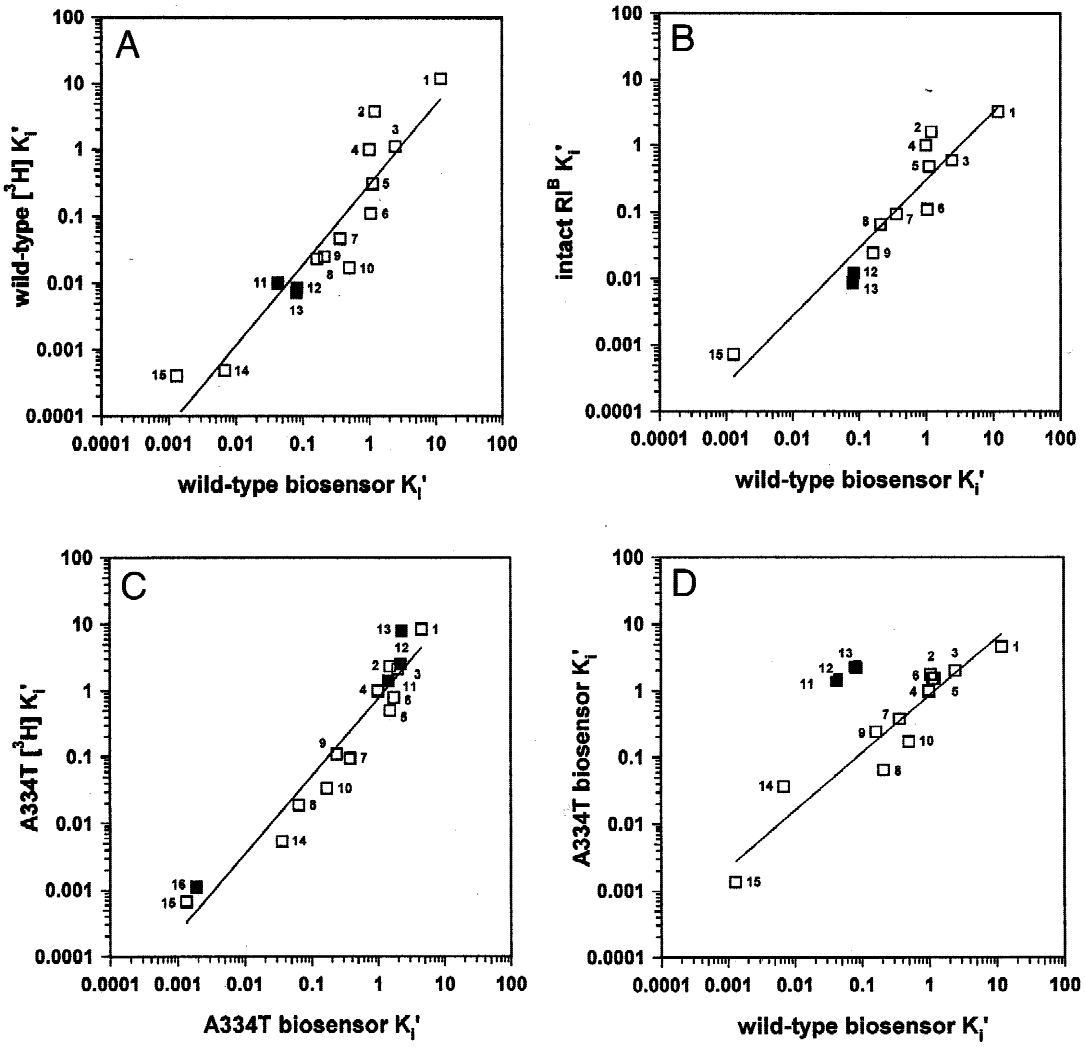

Fig. 7. Comparison of K_i' values for the wild-type and A334T B domains. The K_i' values are from Table 2. The [^{3}H] and biosensor assays for determining K_i' values refer to the equilibrium [^{3}H]cAMP-binding and the biosensor initial rate assays described in Materials and methods. Wild-type and A334T refer to the isolated wild-type and A334T B domains. Intact RI^B refers to the B domain in intact rabbit skeletal muscle RIα. The numbers beside each square indicate the K_i' values for the corresponding compound listed in Table 2. Closed squares represent cGMP analogs. Open squares represent all other cyclic nucleotides. Linear regressions were done with all data points in each panel except for **D**, where compounds 11, 12, and 13 were excluded. Slopes and correlation coefficients for each dataset are stated in the text.

tended to be dimeric. Prolonged storage at 4 °C resulted in the formation of high molecular weight aggregates with altered kinetic properties. To maintain the monomeric form of the B domain and a single kinetic cyclic nucleotide-binding species of the protein, aliquots of B domain were incubated with 20 mM β-mercaptoethanol before each use.

Generation of cUMP-exchanged B domain

To minimize the contribution of bound cyclic nucleotide in inhibition assays, the cIMP was displaced with the lower affinity cUMP through a series of exchange and desalting steps. Cyclic IMP-saturated B domain (100 μL at 70 μM) was incubated with an equal volume of 0.2 M cUMP in KPE for 30 min at 30 °C. Cyclic nucleotides were separated from the B domain by chromatography on a 1 × 40 cm column of Sephadex G-25 superfine equilibrated in 50 mM potassium phosphate, 1 mM EDTA pH 6.8. One milliliter fractions were collected, and those containing B domain were identified by protein dye-binding assay (BioRad, Hercules, California). Peak fractions were pooled and concentrated to 100 μL with Amicon Centriprep 10 and Centricon concentrators. The cUMP exchange was repeated as above. After the second exchange and chromatography, approximately 80% of the B domain was recovered as determined by [^{3}H]cAMP-binding activity. Reversed-phase analysis of cyclic nucleotide content of the boiled aliquots of doubly exchanged B domain according to the method of Krstulovic et al. (1979) showed that the cIMP concentration was less than 5% of the B domain concentration. The effect of cIMP removal was easily demonstrated by an increased apparent association rate constant as determined by biosensor analysis. The molar

ratio of cUMP to B domain in these preparations was at least 1:4, but never more than 1:1.

Determination of cyclic nucleotide K_i' values for the isolated WT B domain using the [^{3}H]cAMP equilibrium binding assay

Wild-type (10 nM) or A334T B domain was incubated in the presence of 50 mM potassium phosphate, pH 6.8, 1 mM EDTA, 2 M NaCl, 0.01% Triton X-100, 0.4 μM [^{3}H] cAMP (8.2×10^{-5} pmol/dpm) and increasing concentrations of competitor nucleotide for 45 min at 30 °C. Samples were diluted with ice-cold KPE (10 mM potassium phosphate pH 6.8, 1 mM EDTA) and immediately filtered over Millipore HAWP nitrocellulose. Filters were washed with KPE, dried, and the protein-bound [^{3}H]cAMP was measured in a scintillation counter. Relative inhibition constants (K_i') where $K_i' = K_i^{\mathrm{cAMP}}/K_i^{\mathrm{analog}}$ were calculated according to (Døskeland et al., 1983). All determinations were performed in duplicate and agreed to within ±20% of the mean.

Biosensor instrumentation

Experiments were done with either a single well IAsys or a dual well IAsys Plus (Affinity Sensors, Franklin, Massachusetts). All manipulations with the 200 μL capacity single-well system were done at 30 °C. Because the 80 μL capacity dual-well system of the IAsys Plus was more sensitive to evaporation, experiments with this instrument were done at 25 °C. The temperature at which kinetic parameters were determined is therefore indicated. Protocols are given only for the indicated instrument, and volume adjustments are necessary to adapt the protocol to the other instrument. Comparison of K_i' data from the two instruments was permissible because these values represented ratios of inhibition constants and are therefore temperature independent.

Immobilization of 8-aminohexylamino cAMP onto the biosensor cuvette

8-Aminohexylamino-cAMP (AHA-cAMP) was immobilized through its free ω-amino group to an IAsys carboxymethyldextran (CMD) cuvette (Affinity Sensors) based on the manufacturer's instructions. All reactions were done at 30 °C. Unless indicated, buffer additions to the cuvette were 200 μL for single-well cuvettes. Buffer exchanges were accomplished by aspiration of the cuvette contents before addition of the next reagent. The CMD cuvette was activated for 10 min with 0.4 M 1-ethyl-3-(3-dimethylaminopropyl) carbodiimide (EDC) and 0.1 M *N*-hydrosuccinimide (NHS) followed by three washes with water. The cuvette was equilibrated 2 min with 50 μL of 50 mM sodium bicarbonate, pH 8.5. To this was added 50 μL of 2.8 mM AHA-cAMP. After a 10 min incubation, the cuvette was washed three times with water to remove unreacted AHA-cAMP. Remaining activated sites in the cuvette were blocked with 1 M ethanolamine pH 8.5 for 2 min and then washed three times with water. The maximum extent of B domain binding (R_{max}) yielded a signal on the IAsys from 500 to 1,200 arc-s, which equated to a density of 3.8 to 7.5 pmol of binding sites as calculated using a cuvette constant of 200 arc-s for 1 ng/mm^2 bound protein for the carboxymethyl dextran cuvette, a cuvette surface area of 18 mm^2, and a mass of 14,380 kDa for the isolated B domain.

Determination of kinetic rate and equilibrium constants

The determination of rate and equilibrium constants using biosensor data has been described in detail by others (reviewed in Hall & Winzor, 1998). All manipulations were carried out at 30 °C. The AHA-cAMP single-well cuvette containing 200 μL of Buffer A (150 mM NaCl, 50 mM potassium phosphate (pH 6.8), 1 mM EDTA, 0.01% Triton X-100) was incubated in the IAsys for at least 4 min or until the baseline stabilized. One to 30 μL of B domain was added to give a final concentration range of between 1 and 200 nM as indicated in the results. The change in arc-s, reflecting the apparent on-rate (k_{on}) of unliganded B domain with the immobilized AHA-cAMP, was monitored at 1 s intervals. The maximum amount of data in the first 3 min of association was used that would allow fitting to a single phase k_{on} as determined by random distribution of error of the fitted curve relative to experimental data using FASTFIT software (Affinity Sensors). The dissociation rate constant (k_d^{on}) and association rate constant (k_a^{on}) were calculated by linear regression of a plot of k_{on} vs. the concentration of free B domain (C) using the relationship:

$$k_{on} = k_d + k_a \cdot C \tag{1}$$

At least four different B domain concentrations (except for one low-range wild-type experiment that used only three) were used for each association experiment. Individual experiments were used only when the standard deviation of each kinetic constant for that experiment was <25% of the mean. Alternatively, the k_a was determined from plots of initial rate measurements vs. B domain concentration (Edwards & Leatherbarrow, 1997) using the following relationship:

$$\frac{dR}{dt} = k_a \cdot R_{max} \cdot C \tag{2}$$

where R_{max} is the maximum arc-s achieved upon saturation of the cuvette with B domain. The initial rate (dR/dt) was determined from linear regression of the first 15 to 60 s of association data at each concentration of B domain using FASTFIT. To determine k_d^{diss}, loss of B domain bound to immobilized AHA-cAMP was monitored after the addition of 1 μL of 12.4 mM cAMP to the cuvette. The dissociation curve was fitted to either single- or double-phase dissociation kinetics using FASTFIT. Equilibrium dissociation constants were derived from either the k_{on}-determined rate constants ($K_d^{kin} = k_d^{on}/k_a^{on}$), or from equilibrium binding data at various concentrations of B domain (K_d^{eq}) using FASTFIT. The K_d^{eq} was calculated from the scatchard plots of R/C vs. R, where R is the maximum extent of arc-s achieved at equilibrium for a given concentration (C) of B domain. Extents were calculated from single-phase k_{on} data. All kinetic constants were reported ± standard error of the mean.

Cuvette regeneration

After every association/dissociation, the single-well cuvette was regenerated with two 15 s washes of 8 M guanidine HCl, followed by two 15 s washes of 1 M formic acid. The cuvette was then washed three times with Buffer A and allowed to equilibrate for the next measurement. The longest lived cuvette was regenerated up to 500 times with a progressive loss of binding capacity of no more

than 50% over the life of the cuvette. The formic acid washes were eliminated for the dual well cuvette in order to increase its longevity.

Biosensor competition assay

The following procedure is designed for the dual-well cuvette system. Use of the two-well system allowed simultaneous duplicate measurements. All cyclic nucleotide inhibitor stock solutions and serial dilutions were made in water and were stored at −70 °C until use. Concentrations of stock solutions were determined from extinction coefficients for each analog. Ten microliter aliquots of inhibitor were added to 188 μL of Buffer A and 2 μL of 1.5 μM B domain to give a final concentration of ~15 nM. The mixture was equilibrated for 30 min at 25 °C. Ninety microliters of this mix was added to each well of a dual-well cuvette after establishment of stable baselines in the presence of 80 μL of Buffer A and 5 μL of water. Association data were accumulated simultaneously from both wells for 2 min at one to five readings per second. Sometimes the first few seconds of data needed to be discarded because of baseline fluctuations caused by the buffer change. The K_i values were calculated by curve fitting of dR/dt vs. $[I]_t$ plots as described above. Relative inhibition constants were calculated as the $K_i^{\mathrm{cAMP}}/K_i^{\mathrm{analog}}$.

Single-well experiments were done under slightly different conditions. Ten microliters of 0.8 μM B domain and 10 μL of varying concentrations of competitor cyclic nucleotide were added to a microfuge tube containing 80 μL of Buffer A and incubated for 30 min at 30 °C to achieve binding equilibrium. The entire contents were transferred to an AHA-cAMP cuvette containing 100 μL of Buffer A and exhibiting a stable baseline. Association data were accumulated for 3 min. The advantage to this approach is that by maintaining some buffer in the cuvette, the dextran surface is stabilized, thus minimizing baseline changes upon addition of the B domain/inhibitor mix. The disadvantage is that the B domain/inhibitor mix is diluted by a factor of 2, which changes the equilibrium between free and bound inhibitor. In our hands, however, we found that this dilution had minimal effect on K_i values.

Determination of inhibition constants using initial rate measurements

The inhibition constant K_i for the reaction $L + I \rightleftarrows LI$ is defined as

$$K_i = \frac{[I][L]}{[LI]} \tag{3}$$

where $[L]$ is the free ligate concentration, $[I]$ is the free inhibitor concentration, and $[LI]$ is the concentration of ligate–inhibitor complex. The term $[LI]$ can be expressed as

$$[LI] = [L]_t - [L] \tag{4}$$

where $[L]_t$ is the concentration of total ligate. The term $[I]$ can be expressed as

$$[I] = [I]_t - [LI] = [I]_t - [L]_t + [L] \tag{5}$$

where $[I]_t$ is the concentration of total inhibitor. Substitution of Equations 4 and 5 into Equation 3 results in

$$K_i = \frac{[L]([I]_t - [L]_t + [L])}{[L]_t - [L]}. \tag{6}$$

Rearrangement of Equation 6 to give a quadratic equation and solving for $[L]$ gives

$$[L] = \frac{[L]_t - [I]_t - K_i + \sqrt{([I]_t - [L]_t + K_i)^2 + 4K_i[L]_t}}{2}. \tag{7}$$

Because $[L]$ is related to the initial rate of association of ligate to the immobilized surface of the biosensor cuvette as shown in Equation 2, Equation 7 can also be expressed as

$$\frac{dR}{dt} = k_a R_{max} \cdot \frac{[L]_t - [I]_t - K_i + \sqrt{([I]_t - [L]_t + K_i)^2 + 4K_i[L]_t}}{2}. \tag{8}$$

If either $k_a \cdot R_{max}$ or $[L]_t$ are known, then K_i can be calculated from nonlinear regression of a plot of dR/dt vs. $[I]_t$ using Equation 8.

Acknowledgments

The authors thank James LaDine (Affinity Sensors) and Friedrich Herberg (Ruhr-Universität Bochum) for critically reading the manuscript and providing expert advice. This work was supported by National Institutes of Health grant R29GM49848 (J.B.S.) and by NSF-OSR9452892 (J.B.S.).

References

Altenhofen W, Ludwig J, Eismann E, Kraus W, Bönigk W, Kaupp UB. 1991. Control of ligand specificity in cyclic nucleotide-gated channels from rod photoreceptors and olfactory epithelium. *Proc Natl Acad Sci USA 88*:9868–9872.

Beebe SJ, Corbin JD. 1986. Cyclic nucleotide-dependent protein kinases. In: Boyer PD, Krebs EG, eds. *Control by phosphorylation, part A*. Orlando, FL: Academic Press, Inc. pp 44–111.

Bowles MR, Hall DR, Pond SM, Winzor DJ. 1997. Studies of protein interactions by biosensor technology: An alternative approach to the analysis of sensorgrams deviating from pseudo-first-order kinetic behavior. *Anal Biochem 244*:133–143.

De Wit RJW, Hoppe J, Stec WJ, Baraniak J, Jastorff B. 1982. Interaction of cAMP derivatives with the "stable" cAMP-binding site in the cAMP-dependent protein kinase type I. *Eur J Biochem 122*:95–99.

Dills WL, Goodwin CD, Lincoln TM, Beavo JA, Bechtel PJ, Corbin JD, Krebs EG. 1979. Purification of cyclic nucleotide receptor proteins by cyclic nucleotide affinity chromatography. *Adv Cyclic Nucleotide Res 10*:198–217.

Døskeland SO, Øgreid D. 1984. Characterization of the interchain and intrachain interactions between the binding sites of the free regulatory moiety of protein kinase I. *J Biol Chem 259*:2291–2301.

Døskeland SO, Øgreid D, Ekanger R, Sturm PA, Miller JP, Suva RH. 1983. Mapping the two intrachain cyclic nucleotide-binding sites of adenosine cyclic 3′,5′-phosphate dependent protein kinase I. *Biochemistry 22*:1094–1101.

Edwards PR, Gill A, Pollard-Knight DV, Hoare M, Buckle PE, Lowe PA, Leatherbarrow RJ. 1995. Kinetics of protein–protein interactions at the surface of an optical biosensor. *Anal Biochem 231*:210–217.

Edwards PR, Leatherbarrow RJ. 1997. Determination of association rate constants by an optical biosensor using initail rate analysis. *Anal Biochem 246*:1–6.

Hall DR, Gorgani NN, Altin JG, Winzor DJ. 1997. Theoretical and experimental considerations of the pseudo-first-order approximation in conventional kinetic analysis of IAsys biosensor data. *Anal Biochem 253*:145–155.

Hall DR, Winzor DJ. 1997. Use of a resonant mirror biosensor to characterize the interaction of carboxypeptidase A with an elicited monoclonal antibody. *Anal Biochem 244*:152–160.

Hall DR, Winzor DJ. 1998. Potential of biosensor technology for the characterization of interactions by quantitative affinity chromatography. *J Chromatogr B 715*:163–181.

Herberg FW, Maleszka A, Eide T, Vossebein L, Tasken K. 2000. Analysis of A-kinase anchoring protein (AKAP) Interaction with protein kinase A (PKA)

regulatory subunits: PKA isoform specificity in AKAP binding. *J Mol Biol 298*:329–339.

Herberg FW, Zimmermann B. 1999. Analysis of protein kinase interactions using biomolecular interaction analysis. In: Hardie DG, ed. *Protein phosphorylation: A practical approach*, 2nd ed., vol. 2. Oxford: Oxford University Press. pp 335–371.

Kalinin NL, Ward LD, Winzor DJ. 1995. Effects of solute multivalence on the evaluation of binding constants by biosensor technology: Studies with concanavalin A and interleukin-6 as partitioning partners. *Anal Biochem 228*:238–244.

Kapphahn MA, Shabb JB. 1997. Contribution of the carboxyl-terminal region of the cAMP-dependent protein kinase type I a regulatory subunit to cyclic nucleotide interactions. *Arch Biochem Biophys 348*:347–356.

Karlsson R. 1994. Real-time competitive kinetic analysis of interactions between low-molecular-weight ligands in solution and surface-immobilized receptors. *Anal Biochem 221*:142–151.

Karlsson R, Fägerstam L, Nilshans H, Persson B. 1993. Analysis of active antibody concentration. Separation of affinity and concentration parameters. *J Immunol Methods 166*:75–84.

Krstulovic AM, Hartwick RA, Brown PR. 1979. Reversed-phase liquid chromatographic separation of 3′,5′-cyclic ribonucleotides. *Clin Chem 25*:235–241.

Mann DA, Motomu K, Maly DJ, Kiessling LL. 1998. Probing low affinity and multivalent interactions with surface plasmon resonance: Ligands for concanavalin A. *J Am Chem Soc 120*:10575–10582.

Morelock MM, Ingraham RH, Betageri R, Jakes S. 1995. Determination of receptor–ligand kinetic and equilibrium binding constants using surface plasmon resonance: Application to the lck SH2 domain and phosphotyrosyl peptides. *J Med Chem 38*:1308–1318.

Myszka DG, Morton TA, Doyle ML, Chaiken IM. 1997. Kinetic analysis of a protein antigen–antibody interaction limited by mass transport on an optical biosensor. *Biophys Chem 64*:127–137.

Nieba L, Krebber A, Plückthun A. 1996. Competition BIAcore for measuring true affinities: Large differences from values determined from binding kinetics. *Anal Biochem 234*:155–165.

Øgreid D, Ekanger R, Suva RH, Miller JP, Døskeland SO. 1989. Comparison of the two classes of binding sites (A and B) of type I and type II cyclic-AMP-dependent protein kinases by using cyclic nucleotide analogs. *Eur J Biochem 181*:19–31.

O'Shannessy DJ, Winzor DJ. 1996. Interpretation of deviations from pseudo-first-order kinetic behavior in the characterization of ligand binding by biosensor technology. *Anal Biochem 236*:275–283.

Rannels SR, Corbin JD. 1980. Two different intrachain cAMP binding sites of cAMP-dependent protein kinases. *J Biol Chem 255*:7085–7088.

Reed RB, Sandberg M, Jahnsen T, Lohmann SM, Francis SH, Corbin JD. 1996. Fast and slow cyclic nucleotide-dissociation sites in cAMP-dependent protein kinase are transposed in type I b cGMP-dependent protein kinase. *J Biol Chem 271*:17570–17575.

Schuck P. 1997. Use of surface plasmon resonance to probe the equilibrium and dynamic aspects of interactions between biological macromolecules. *Annu Rev Biophys Biomol Struct 26*:541–566.

Schuck P, Minton AP. 1996a. Analysis of mass transport-limited binding kinetics in evanescent wave biosensors. *Anal Biochem 240*:262–272.

Schuck P, Minton AP. 1996b. Kinetic analysis of biosensor data: Elementary tests for self-consistency. *Trends Biochem 21*:458–460.

Shabb JB, Buzzeo BD, Ng L, Corbin JD. 1991. Mutating protein kinase cAMP-binding sites into cGMP-binding sites: Mechanism of cGMP selectivity. *J Biol Chem 266*:24320–24326.

Shabb JB, Corbin JD. 1992. Cyclic nucleotide-binding domains in proteins having diverse functions. *J Biol Chem 267*:5723–5726.

Shabb JB, Ng L, Corbin JD. 1990. One amino acid change produces a high affinity cGMP-binding site in cAMP-dependent protein kinase. *J Biol Chem 265*:16031–16034.

Shabb JB, Poteet CE, Kapphahn MA, Muhonen WM, Baker NE, Corbin JD. 1995. Characterization of the isolated cAMP-binding B domain of cAMP-dependent protein kinase. *Protein Sci 4*:2100–2106.

Su Y, Dostmann WRG, Herberg FW, Durick K, Xuong N, Ten Eyck L, Taylor SS, Varughese KI. 1995. Regulatory subunit of protein kinase A: Structure of deletion mutant with cAMP binding domains. *Science 269*:807–813.